

Tethered Olefin Studies of Alkene versus Tetraphenylborate Coordination and Lanthanide Olefin Interactions in Metallocenes

William J. Evans,* Jeremy M. Perotti, Jason C. Brady, and Joseph W. Ziller

Contribution from the Department of Chemistry, University of California, Irvine, California 92697-2025

Received July 12, 2002; E-mail: wevans@uci.edu

Abstract: The tethered olefin cyclopentadienyl ligand, $[(C_5Me_4)SiMe_2(CH_2CH=CH_2)]^-$, forms unsolvated metallocenes, $[(C_5Me_4)SiMe_2(CH_2CH=CH_2)]_2Ln$ ($Ln = Sm, 1; Eu, 2; Yb, 3$), from $[(C_5Me_4)SiMe_2(CH_2CH=CH_2)]K$ and $LnI_2(THF)_2$ in good yield. Each complex in the solid state has both tethered olefins oriented toward the Ln metal center with the $Ln-C$ (terminal alkene carbon) distances 0.2–0.3 Å shorter than the $Ln-C$ (internal alkene carbon) distances. The olefinic $C-C$ bond distances in **2** and **3**, 1.328(4) and 1.328(5) Å, respectively, are normal. Like its permethyl analogue, $(C_5Me_5)_2Sm(THF)_2$, complex **1** reductively couples CO_2 to form the oxalate-bridged dimer $\{[(C_5Me_4)SiMe_2(CH_2CH=CH_2)]_2Sm\}_2(\mu-\eta^2-\eta^2-O_2CCO_2)$, **4**, in which the tethered olefins are noninteracting substituents. Complex **1** reacts with $AgBPh_4$ to form an unsolvated cation that has the option of coordinating $[BPh_4]^-$ or a pendant olefin, a competition common in olefin polymerization catalysis. The structure of $\{[(C_5Me_4)SiMe_2(CH_2CH=CH_2)]_2Sm\}[BPh_4]$, **5**, shows that both pendant olefins are located near samarium rather than the $[BPh_4]^-$ counterion.

Introduction

Alkene coordination to cationic metallocenes is commonly accepted as a key component in both the initiation and propagation of many homogeneous olefin polymerization reactions involving single site catalysts.^{1–16} One of the ongoing issues involving the reactivity of cationic polymerization sites involves the interaction of the metal center with the counteranion vis-à-vis the incoming monomer. We report here on the use of the alkene-substituted cyclopentadienyl ligand, $[(C_5Me_4)SiMe_2(CH_2CH=CH_2)]^-$, to probe metal–olefin versus metal–counteranion interactions in a cationic metallocene environment.

This tethered olefin ligand was chosen since it recently has been useful in providing information related to olefin polymerization.¹⁷ In the prior study, this ligand provided information on a previously undetected type of olefin metalation. This ligand also had the potential to be useful in the study of olefin complexation to cationic centers, since synthetic routes to unsolvated lanthanide-based metallocene cations, $[(C_5Me_5)_2Ln]^+$ and $[(C_5Me_4R)_2Ln]^+$, have been well established.^{18,19} In complexes containing simple C_5R_5 ligands, the $[BPh_4]^-$ counteranions are oriented toward the metal center via the phenyl groups. Formation of analogues with $[(C_5Me_4)SiMe_2(CH_2CH=CH_2)]^-$ would set up a competition between $[BPh_4]^-$ and olefin coordination so that the question of substrate versus counteranion could be examined in a metallocene environment. Lanthanide complexes are appropriate for this study, since they are active in a variety of catalytic processes involving unsaturated hydrocarbons including alkene^{20–27} and diene²⁸ polymerization

- Rappe, A. K.; Skiff, W. M.; Casewit, C. J. *Chem. Rev.* **2000**, *100*, 1435.
- Chen, E. Y.-X.; Marks, T. J. *Chem. Rev.* **2000**, *100*, 1391.
- Coates, G. W. *Chem. Rev.* **2000**, *100*, 1223.
- Margl, P.; Deng, L.; Ziegler, T. *Organometallics* **1998**, *17*, 933.
- Brintzinger, H. H.; Fischer, D.; Mülhaupt, R.; Rieger, B.; Waymouth, R. M. *Angew. Chem., Int. Ed. Engl.* **1995**, *34*, 1143.
- Casey, C. P.; Lee, Y.-T.; Tunge, J. A.; Carpenetti, D. W. *J. Am. Chem. Soc.* **2001**, *123*, 10762.
- Casey, C. P.; Carpenetti, D. W., II. *Organometallics* **2000**, *19*, 3970.
- Casey, C. P.; Fagan, M. A.; Hallenbeck, S. L. *Organometallics* **1998**, *17*, 287.
- Casey, C. P.; Fisher, J. J. *Inorg. Chim. Acta* **1998**, *270*, 5.
- Casey, C. P.; Hallenbeck, S. L.; Wright, M. J.; Landis, C. R. *J. Am. Chem. Soc.* **1997**, *119*, 9680.
- Casey, C. P.; Hallenbeck, S. L.; Pollock, D. W.; Landis, C. R. *J. Am. Chem. Soc.* **1995**, *117*, 9770.
- Schumann, H.; Heim, A.; Demtschuk, J.; Muhle, S. H. *Organometallics* **2002**, *21*, 3323.
- Lin, J.; Wang, Z. *J. Organomet. Chem.* **1999**, *589*, 127.
- Carpentier, J.-F.; Wu, Z.; Lee, C. W.; Strömberg, S.; Christopher, J. N.; Jordan, R. F. *J. Am. Chem. Soc.* **2000**, *122*, 7750.
- Wu, Z.; Jordan, R. F.; Petersen, J. L. *J. Am. Chem. Soc.* **1995**, *117*, 5867.
- Galakhov, M. V.; Heinz, G.; Royo, P. *J. Chem. Soc., Chem. Commun.* **1998**, 17.

- Evans, W. J.; Brady, J. C.; Ziller, J. W. *J. Am. Chem. Soc.* **2001**, *123*, 7711.
- Evans, W. J.; Seibel, C. A.; Ziller, J. W. *J. Am. Chem. Soc.* **1998**, *120*, 6745.
- Evans, W. J.; Davis, B. L.; Ziller, J. W. *Inorg. Chem.* **2001**, *40*, 6341.
- Evans, W. J.; Bloom, I.; Hunter, W. E.; Atwood, J. L. *J. Am. Chem. Soc.* **1981**, *103*, 6507.
- Evans, W. J.; DeCoster, D. M.; Greaves, J. *Organometallics* **1996**, *15*, 3210.
- Evans, W. J.; DeCoster, D. M.; Greaves, J. *Macromolecules* **1995**, *28*, 7929.
- Jeske, G.; Schock, L. E.; Swepstone, P. N.; Schumann, H.; Marks, T. J. *J. Am. Chem. Soc.* **1985**, *107*, 8103.
- Watson, P. L.; Parshall, G. W. *Acc. Chem. Res.* **1985**, *18*, 51.
- Evans, W. J.; Ulibarri, T. A.; Chamberlain, L. R.; Ziller, J. W.; Alvarez, D., Jr. *Organometallics* **1990**, *9*, 2124.
- Yasuda, H.; Ihara, E. *Adv. Polym. Sci.* **1997**, *133*, 53.
- Boffa, L. S.; Novak, B. M. *Macromolecules* **1997**, *30*, 3494.
- Evans, W. J.; Giarikos, D. G.; Ziller, J. W. *Organometallics* **2001**, *20*, 5751.

and alkene hydrogenation,^{29–35} hydroamination,^{36–39} and hydrosilylation.^{40–43}

Preparation of the necessary lanthanide metallocene precursors to the $[(C_5Me_4R)_2Ln]^+$ cations, namely $[(C_5Me_4)SiMe_2(CH_2CH=CH_2)]_2Ln$ ($Ln = Sm, Eu, Yb$), has proven to be independently interesting. These neutral metallocenes have allowed the investigation of lanthanide olefin interactions, a subject on which few data are available.^{6–13,44–52,81}

Experimental Section

The complexes described in the following are extremely air and moisture sensitive. Syntheses and manipulations of these compounds were conducted under nitrogen or argon with rigorous exclusion of air and water by Schlenk, vacuum line, and glovebox techniques. THF and diethyl ether were dried over activated alumina and sieves. Toluene and hexanes were dried over Q-5 and molecular sieves. Benzene-*d*₆ was distilled over an NaK alloy and benzophenone. $(C_5Me_4H)SiMe_2(CH_2CH=CH_2)$,¹⁷ $LnI_2(THF)_2$ ($Ln = Sm, Eu, Yb$),⁵³ and $AgBPh_4$ ⁵⁴ were prepared as previously described. KH was purchased from Aldrich and washed with hexanes before use. NMR spectra were measured using a Bruker 400 MHz spectrometer. IR samples were prepared as thin films, and spectra were obtained using an ASI ReactIR 1000. Elemental analysis was provided by Desert Analytics, and complexometric analyses were performed as previously described.⁵⁵

$[(C_5Me_4)SiMe_2(CH_2CH=CH_2)]_2K$. $(C_5Me_4H)SiMe_2(CH_2CH=CH_2)$ (2.0 g, 9.07 mmol) was added to a slurry of KH (360 mg, 8.98 mmol) in 50 mL of diethyl ether. The mixture was stirred for 24 h during which time a white solid precipitate formed. White $[(C_5Me_4)SiMe_2(CH_2CH=CH_2)]_2K$ (1.89 g, 80%) was collected by filtration, dried under vacuum, and used without further purification.

- (29) Evans, W. J.; Engerer, S. C.; Piliero, P. A.; Wayda, A. L. In *Fundamental Research in Homogeneous Catalysis*; Tsutsui, M., Ed.; Plenum Publishing Corp.: New York, 1979; Vol. 3, pp 941–952.
- (30) Evans, W. J.; Engerer, S. C.; Piliero, P. A.; Wayda, A. L. *J. Chem. Soc., Chem. Commun.* **1979**, 1007.
- (31) Evans, W. J.; Bloom, I.; Hunter, W. E.; Atwood, J. L. *J. Am. Chem. Soc.* **1983**, *105*, 1401.
- (32) Jeske, G.; Lauke, H.; Mauermann, H.; Schumann, H.; Marks, T. J. *J. Am. Chem. Soc.* **1985**, *107*, 8111.
- (33) Molander, G. A.; Hoberg, J. O. *J. Org. Chem.* **1992**, *57*, 3266.
- (34) Komarov, I. V.; Denisenko, V. E.; Kornilov, M. Y. *Tetrahedron* **1996**, *50*, 6921.
- (35) Roesky, P. W.; Denninger, U.; Stern, C. L.; Marks, T. J. *Organometallics* **1997**, *16*, 4486.
- (36) Tian, S.; Arredondo, V. M.; Stern, C. L.; Marks, T. J. *Organometallics* **1999**, *18*, 2568.
- (37) Arredondo, V. M.; McDonald, F. E.; Marks, T. J. *Organometallics* **1999**, *18*, 1949.
- (38) Molander, G. A.; Dowdy, E. D. *J. Org. Chem.* **1998**, *63*, 8983.
- (39) Li, Y.; Marks, T. J. *J. Am. Chem. Soc.* **1998**, *120*, 1757.
- (40) Voskoboinikov, A. Z.; Shestakova, A. K.; Beletskaya, I. P. *Organometallics* **2001**, *20*, 2794.
- (41) Fu, P. F.; Bard, L.; Li, Y.; Marks, T. J. *J. Am. Chem. Soc.* **1995**, *117*, 7157.
- (42) Molander, G. A.; Julius, M. *J. Org. Chem.* **1992**, *57*, 6347.
- (43) Sakakura, T.; Lautenschlager, H.; Tanaka, M. *J. Chem. Soc., Chem. Commun.* **1991**, 40.
- (44) Burns, C. J.; Andersen, R. A. *J. Am. Chem. Soc.* **1987**, *109*, 915.
- (45) Schultz, M.; Burns, C. J.; Schwartz, D. J.; Andersen, R. A. *Organometallics* **2000**, *19*, 781.
- (46) Evans, W. J.; Coleson, K. M.; Engerer, S. C. *Inorg. Chem.* **1981**, *20*, 4320.
- (47) Evans, W. J. *High-Energy Processes in Organometallic Chemistry*; Suslick, K. S., Ed.; ACS Symposium Series 333; American Chemical Society: Washington, DC, 1987; p 278.
- (48) Schilling, J. B.; Beauchamp, J. L. *J. Am. Chem. Soc.* **1988**, *110*, 15.
- (49) Cornehl, H. H.; Heinemann, C.; Schröder, D.; Schwarz, H. *Organometallics* **1995**, *14*, 992.
- (50) Heinemann, C.; Schröder, D.; Schwarz, H. *Chem. Ber.* **1994**, *127*, 1807.
- (51) Berg, D. J.; Louie, A.; Fei, X. Canadian Society of Chemistry 2002 National Meeting: Vancouver, B.C., June 2002, #764.
- (52) Schumann, H.; Heim, A.; Karasiak, D.; Demtschuk, M.; Muhle, S. H. Canadian Society of Chemistry 2002 National Meeting: Vancouver, B.C., June 2002, #510.
- (53) Namy, J. L.; Girard, P.; Kagan, H. B. *Nouv. J. Chim.* **1981**, *5*, 479.
- (54) Jordan, R. F.; Echols, S. F. *Inorg. Chem.* **1987**, *26*, 383.
- (55) Evans, W. J.; Grate, A. W.; Levan, K. R.; Bloom, I.; Peterson, T. T.; Doedens, R. J.; Zhang, H.; Atwood, J. L. *Inorg. Chem.* **1986**, *25*, 3614.

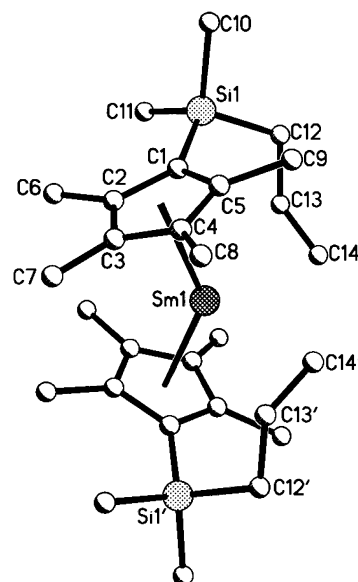


Figure 1. Ball and stick figure of $[(C_5Me_4)SiMe_2(CH_2CH=CH_2)]_2Sm$, **1**.

$[(C_5Me_4)SiMe_2(CH_2CH=CH_2)]_2Sm$, **1.** A dark blue solution of $SmI_2(THF)_2$ (127 mg, 0.232 mmol) in 3 mL of THF was added to a slurry of $[(C_5Me_4)SiMe_2(CH_2CH=CH_2)]_2K$ (122 mg, 0.473 mmol) in 10 mL of THF. The color immediately changed to dark green, and a white precipitate formed. The reaction was stirred for 4 h and centrifuged to remove the insoluble material. Removal of THF under vacuum gave oily dark solids which were extracted with hexanes to produce a dark green solution and dark insoluble material. The reaction was centrifuged, and the dark green solution was separated. The dark solids were extracted with hexanes 2 times, and the combined hexane solutions were evaporated to yield **1** (0.90 mg, 66%) as a dark green waxy solid. Crystals suitable for X-ray diffraction were grown from toluene at -32 °C (Figure 1). 1H NMR (C_6D_6 , 25 °C): δ -0.99 (s, 12H), 0.51 (s, 12H), 6.21 (s, 12H), 10.22 (s, 4H), 28.4 (s, 2H), 38.4 (s, 2H), 42.4 (s, 2H). $\mu_{eff} = 3.76$ at 298 K. IR (thin film): 3076w, 2964s, 2914s, 2860s, 1629s, 1444m, 1390w, 1328w, 1251s, 1220m, 1154m, 1096w, 1023m, 988w, 953w, 930w, 892m, 822m, br, 699w. Anal. Calcd for $C_{28}H_{46}Si_2Sm$: C, 57.08; H, 7.89; Sm, 25.51. Found: C, 56.99; H, 7.86; Sm, 25.55.

$[(C_5Me_4)SiMe_2(CH_2CH=CH_2)]_2Eu$, **2.** A fluorescent-light green solution of $EuI_2(THF)_2$ (87.0 mg, 0.158 mmol) in 3 mL of THF was reacted with $[(C_5Me_4)SiMe_2(CH_2CH=CH_2)]_2K$ (82.0 mg, 0.317 mmol) in 5 mL of THF to form **2** as a red waxy solid (65.3 mg, 70%). X-ray quality crystals were obtained by cooling a concentrated hexanes solution of **2** to -32 °C (Figure 2). 1H NMR (C_6D_6 , 25 °C, broad singlets $\Delta\nu_{1/2} = 24$ Hz): δ -0.03 , 0.28, 0.88, 1.10, 1.79, 1.89, 3.25. IR (thin film): 3076w, 2964s, 2914s, 2860s, 1629s, 1559w, 1444m, 1320m, 1251s, 1220m, 1154m, 1108w, 1038m, 984m, 953w, 930w, 891m, 834m, br, 721w, 699w. Anal. Calcd For $C_{28}H_{46}Si_2Eu$: C, 56.92; H, 7.86; Eu, 25.72. Found: C, 56.66; H, 7.82; Eu, 25.74.

$[(C_5Me_4)SiMe_2(CH_2CH=CH_2)]_2Yb$, **3.** A yellow-green solution of $YbI_2(THF)_2$ (68.0 mg, 0.119 mmol) in 3 mL of THF was reacted with $[(C_5Me_4)SiMe_2(CH_2CH=CH_2)]_2K$ (65.0 mg, 0.251 mmol) in 5 mL of THF to form **3** as a green waxy solid (65.5 mg, 90%). Crystals suitable for X-ray diffraction were grown from toluene at -32 °C (Figure 3). 1H NMR (C_6D_6 , 25 °C): δ 0.282 (s, 12H) $SiMe_2$, 1.78 (d, $J = 8.4$ Hz, 4H) $CH_2CH=CH_2$, 2.04 (s, 12 H) ring *Me*, 2.14 (s, 12H) ring *Me*, 4.51 (d, $J = 16.8$ Hz, 2H) $CH_2CH=CH_2$, 4.85 (d, $J = 12.4$ Hz, 2H) $CH_2CH=CH_2$, 6.02 (m, 2H) $CH_2CH=CH_2$. ^{13}C NMR (C_6D_6 , 25 °C): δ 1.20 $SiMe_2$, 11.6 ring *Me*, 14.1 ring *Me*, 28.2 $CH_2CH=CH_2$, 107.1 ring C–Si, 107.9 $CH_2CH=CH_2$, 118.9 ring C–Me, 122.9 ring C–Me, 147.6 $CH_2CH=CH_2$. IR (thin film): 3076w, 2964s, 2914s, 2860s, 1629s, 1559w, 1444m, 1390w, 1328m, 1251s, 1220m, 1154m, 1108w,

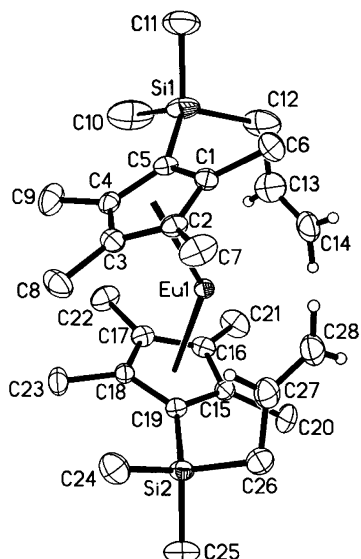


Figure 2. Thermal ellipsoid plot of $[(C_5Me_4)SiMe_2(CH_2CH=CH_2)_2]_2Eu$, **2**, with ellipsoids drawn at the 50% probability level.

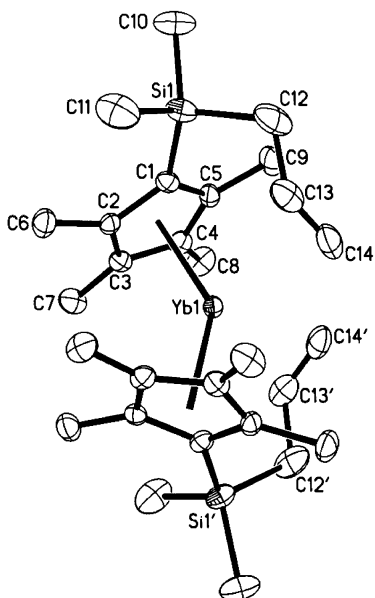


Figure 3. Thermal ellipsoid plot of $[(C_5Me_4)SiMe_2(CH_2CH=CH_2)_2]_2Yb$, **3**, with ellipsoids drawn at the 50% probability level.

1023m, 988m, 953w, 930w, 892m, 834m, br, 687w. Anal. Calcd For $C_{28}H_{46}Si_2Yb$: C, 54.96; H, 7.59; Yb, 28.28. Found: C, 54.87; H, 7.39; Yb, 28.11.

$\{[(C_5Me_4)SiMe_2(CH_2CH=CH_2)_2Sm]_2(\mu-\eta^2:\eta^2-O_2CCO_2)\}$, **4**. A round-bottom flask fitted with a high vacuum greaseless stopcock containing **1** (225 mg, 0.382 mmol) in 20 mL of hexanes was attached to a high vacuum line and evacuated to the vapor pressure of the solvent. The flask was charged with 1 atm of CO_2 , and the dark green color changed to yellow/orange in 2 min. The reaction was stirred for 1 h, after which the solvent was removed leaving **4** (230 mg, 95%) as an orange solid. X-ray quality crystals were obtained by cooling a saturated hexane solution of **4** to $-32^\circ C$. 1H NMR (C_6D_6 , $25^\circ C$): δ -3.67 (s, 12H) $SiMe_2$, -1.19 (d, $J = 8.4$ Hz, 4H) $CH_2CH=CH_2$, -0.589 (s, 12H) ring *Me*, 4.00 (d, $J = 15.6$ Hz, 2H) $CH_2CH=CH_2$, 4.22 (d, $J = 12.0$ Hz, 2H) $CH_2CH=CH_2$, 4.73 (m, 2H) $CH_2CH=CH_2$, 6.69 (s, 12H) ring *Me*. ^{13}C NMR (C_6D_6 , $25^\circ C$): δ -4.89 $SiMe_2$, 15.1 ring *Me*, 22.0 ring *Me*, 28.1 $CH_2CH=CH_2$, 111.4 ring C–Si, 112.1 $CH_2CH=CH_2$, 122.5 ring C–Me, 133.5 $CH_2CH=CH_2$, 134.6 ring C–*Me*. IR (thin film): $3076w$, $2964s$, $2914s$, $2860s$, $1653s$, $1652s$, $1444w$, $1309m$,

$1258s$, $1220w$, $1154w$, $1096s$, $1023s$, $988m$, $953w$, $930w$, $891m$, $834s$, $803s$, $699w$. Anal. Calcd for $C_{58}H_{92}O_4Si_4Sm_2$: C, 55.01; H, 7.34; Sm, 23.75. Found: C, 53.94; H, 7.26; Sm, 23.55.

$\{[(C_5Me_4)SiMe_2(CH_2CH=CH_2)_2Sm][BPh_4]\}$, **5**. A dark green solution of **1** (68 mg, 0.115 mmol) in 8 mL of toluene was added to a slurry of $AgBPh_4$ (49 mg, 0.115 mmol) in 5 mL of toluene wrapped in aluminum foil. The reaction was stirred for 12 h, during which time the color changed to dark red/orange and a black solid precipitate formed. The reaction was centrifuged to remove the insoluble material leaving a red/orange solution. The toluene was removed leaving **5** as a dark red oily solid (70 mg, 67%). Slow evaporation of a warm toluene solution of **5** produced crystals suitable for X-ray diffraction studies. 1H NMR (C_6D_6 , $25^\circ C$): δ -1.33 (broad singlet) ring *Me*, 7.78 (broad singlet) *BPh*₄. IR (thin film): $2964s$, $2918s$, $2860s$, $1629w$, $1594w$, br, $1482w$, $1432m$, $1258s$, $1154w$, $1096s$, $1023s$, $953w$, $892w$, $834s$, $803s$, $745m$, $703s$. Anal. Calcd for $C_{52}H_{66}BSi_2Sm$: C, 68.75; H, 7.34; Sm, 16.55. Found: C, 68.12; H, 7.33; Sm, 16.47.

Reaction of 1 With Ethylene. A dark green solution of **1** (25 mg, 0.042 mmol) in 15 mL of hexane was added to a round-bottom flask equipped with a greaseless high vacuum stopcock. The solution was evacuated to the boiling point of the solvent, and 1 atm of ethylene was introduced. The dark green color remained, and noticeable amounts of colorless precipitate formed within 3 min. The reaction was continued until ethylene uptake ceased (1 h) and copious amounts of colorless solids were observed. The reaction was quenched with D_2O , and the slurry was filtered yielding a colorless solid. The organic solution was separated and analyzed by GC/MS. The solid was washed with 5% HCl (3×5 mL), followed by washing with 2-propanol (3×15 mL). The resulting white solid was dried under vacuum leaving 390 mg of a fluffy white solid. mp = $138^\circ C$. The only major product in the organic filtrate was the diene $(C_5Me_4D)SiMe_2(CH_2CH=CH_2)$.

X-ray Data Collection, Structure Solution, and Refinement for 1. A green crystal of approximate dimensions $0.14 \times 0.16 \times 0.26$ mm³ was mounted on a glass fiber and transferred to a Bruker CCD platform diffractometer. The SMART⁵⁶ program package was used to determine the unit-cell parameters and for data collection (25 s/frame scan time for a sphere of diffraction data). The raw frame data was processed using SAINT⁵⁷ and SADABS⁵⁸ to yield the reflection data file. Subsequent calculations were carried out using the SHELXTL⁵⁹ program. The diffraction symmetry was $2/m$, and the systematic absences were consistent with the monoclinic space groups $C2$, Cm , or $C2/m$. It was later determined that the noncentrosymmetric space group $C2$ was correct.

The structure was solved by direct methods and refined on F^2 by full-matrix least-squares techniques. The analytical scattering factors⁶⁰ for neutral atoms were used throughout the analysis. Hydrogen atoms were included using a riding model. The molecule was located on a 2-fold rotation axis. There was one molecule of toluene solvent present per formula unit. The toluene was also located on a 2-fold axis. The absolute structure was assigned by refinement of the Flack parameter.⁶¹ Similar experimental methods were used for all X-ray experiments. Structural details are in the Supporting Information.

Results

The Cyclopentadienyl Potassium Precursor. $(C_5Me_4H)-SiMe_2(CH_2CH=CH_2)$ is readily deprotonated with KH in diethyl ether to make $[(C_5Me_4)SiMe_2(CH_2CH=CH_2)]K$. The unsolvated

(56) SMART Software Users Guide, Version 5.1; Bruker Analytical X-ray Systems, Inc.: Madison, WI, 1999.

(57) SAINT Software Users Guide, Version 6.0; Bruker Analytical X-ray Systems, Inc.: Madison, WI, 1999.

(58) Sheldrick, G. M. SADABS, version 2.03; Bruker Analytical X-ray Systems, Inc.: Madison, WI, 2000.

(59) Sheldrick, G. M. SHELXTL, version 5.10; Bruker Analytical X-ray Systems, Inc.: Madison, WI, 1999.

(60) International Tables for X-ray Crystallography 1992, Vol. C.; Kluwer Academic Publishers: Dordrecht, The Netherlands.

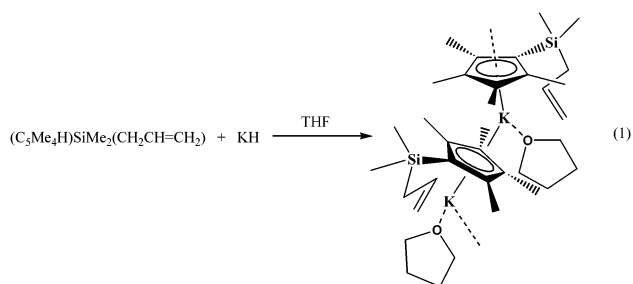
(61) Flack, H. D. Acta Crystallogr. **1983**, A39, 876.

Table 1. Comparison of Alkene Resonances for [(C₅Me₄)SiMe₂(CH₂CH=CH₂)₂Yb (**3**), **3** + THF, **3** + DME, **3** + Pyridine, **3** + 2,2-Bipyridine, C₅Me₄(SiMe₂CH₂CH=CH₂)H, [(C₅Me₄)SiMe₂(CH₂CH=CH₂)Y(CH₂SiMe₃)₂(THF)₂ (**6**), {(C₅Me₄)SiMe₂(CH₂CH=CH₂)Y(O₂CCH₂SiMe₃)₂ (**7**), [(C₅Me₄)SiMe₂(CH₂CH=CH₂)₂Sm (**1**), **1** + THF, {(C₅Me₄)SiMe₂(CH₂CH=CH₂)₂Sm}₂(μ-η²: η²-O₂CCO₂) (**4**), (C₅Me₅)₂Y[η¹-CH₂CH₂C(CH₃)₂CH=CH₂] (**11**), (C₅Me₅)₂Y[η¹-CH₂CH₂C(CH₃)₂CH=CH₂](THF) (**11**·THF), and 3,3-Dimethyl-1,4-pentadiene

compound	¹ H NMR		¹³ C NMR	
	δ(=CH ₂)	δ(-CH=)	δ(=CH ₂)	δ(-CH=)
3	4.51 (d), 4.85 (d)	6.02 (m)	107.9	147.6
3 + THF	4.82 (d), 4.92 (dd)	5.94 (m)	111.0	140.5
3 + DME	4.70 (d), 4.90 (dd)	5.98 (m)	111.1	140.1
3 + pyridine	4.95 (m)	5.95 (m)	112.0	138.1
3 + 2,2-bipyridine	4.50 (d), 4.58 (d)	4.80 (m)	112.0	136.0
C ₅ Me ₄ (SiMe ₂ CH ₂ CH=CH ₂)H	4.90 (m)	5.73 (m)	113.7	135.5
6	4.94 (m)	5.83 (m)	113.5	136.1
7	5.01 (m)	5.99 (m)	112.7	136.5
1	28.4 (s), 38.4 (s)	42.4 (s)	<i>a</i>	<i>a</i>
1 + THF	26.6 (s), 32.9 (s)	36.6 (s)	<i>a</i>	<i>a</i>
4	4.22 (d)	4.73 (s)	112.1	133.5
11	3.76 (d), 5.14 (d)	6.78 (dd)	110.5	161.1
11 ·THF	4.75 (m)	5.78 (dd)	108.4	150.7
3,3-dimethyl-1,4-pentadiene	4.87 (d), 4.92 (d)	5.74 (dd)	111.1	146.1

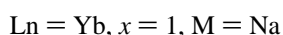
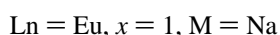
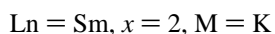
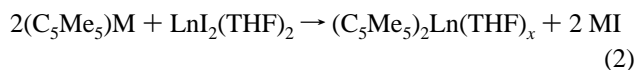
^a Due to the paramagnetism of **1**, the ¹³C NMR was uninformative.

potassium salt is insoluble in alkanes, arenes, and diethyl ether, but it is partially soluble in THF. When the KH deprotonation is conducted in THF, {[(C₅Me₄)SiMe₂(CH₂CH=CH₂)]K(THF)}_n is obtained,⁶² as shown in eq 1. The cyclopentadienyl



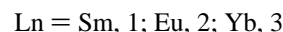
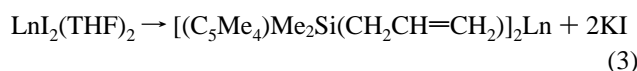
rings in the polymeric structure of this complex are all bridging such that they generate bent metallocene subunits to which THF is attached. The tethered olefin appears to be oriented toward the potassium, but the K···C(internal alkene carbon) distance of 3.58(3) Å and the K···C(terminal alkene carbon) length of 4.20(3) Å are long.

Samarium, Europium, and Ytterbium Metallocenes. The formation of lanthanide metallocenes of [(C₅Me₄)SiMe₂(CH₂CH=CH₂)₂]⁻ was attempted following the synthesis used successfully for the C₅Me₅ analogues, eq 2.^{63–65}



[(C₅Me₄)SiMe₂(CH₂CH=CH₂)]K reacts instantly with LnI₂(THF)₂ in THF to make [(C₅Me₄)SiMe₂(CH₂CH=CH₂)₂Ln (Ln

= Sm, **1**; Eu, **2**; Yb, **3**), eq 3, in a reaction analogous to eq 2.



Complexes **1–3** are very soluble in alkanes and like their C₅Me₅ analogues they can be separated from the byproduct KI by hydrocarbon extraction. A major difference between complexes **1–3** and the analogous C₅Me₅ systems is that **1–3** are isolated in an unsolvated state. In contrast, the permethyl complexes, (C₅Me₅)₂Ln, solvate readily and removal of coordinated THF is not easy.^{45,66}

Complexes **1–3** are intensely colored as is typical of divalent lanthanide metallocenes.⁶⁵ The dark green color of **1** is similar to that of unsolvated (C₅Me₅)₂Sm. Addition of THF to **1** changes the color to a dark brown, whereas (C₅Me₅)₂Sm(THF)₂ is purple. The dark red color of **2** is similar to that of (C₅Me₅)₂Eu and (C₅Me₅)₂Eu(THF). The dark green color of **3** is like that of (C₅-Me₄H)₂Yb and (1,3-^tBu₂C₅H₃)₂Yb, but (C₅Me₅)₂Yb is dark black/brown and (C₅Me₅)₂Yb(THF) is red. The infrared spectra of complexes **1**, **2**, and **3** are essentially identical. Each spectrum contains peaks that can be assigned to the major functional groups: 2964, 2914, and 2860 cm⁻¹ were assigned to ring methyl C–H stretches, 1629 cm⁻¹ is assigned to the C=C stretch of the tethered alkene, and 1251 cm⁻¹ is assigned to the Si–CH₃ stretch.

Initially, NMR spectroscopy was used to probe for coordination of the pendant olefins to the metal centers in the [(C₅Me₄)SiMe₂(CH₂CH=CH₂)₂Ln complexes. Data are summarized in Table 1. The ¹H NMR spectrum of diamagnetic **3** in C₆D₆ is free of THF, but gives no compelling evidence for metal–alkene interactions. A pair of doublets centered at δ 4.51 and 4.85 is observed for the protons of the terminal alkene carbon, and a multiplet at δ 6.02 is found for the proton on the internal alkene carbon. These peaks are only slightly shifted from those found in [(C₅Me₄)SiMe₂(CH₂CH=CH₂)]Y(CH₂-

(62) Evans, W. J.; Brady, J. C.; Giarikos, D. G.; Fujimoto, C. H.; Ziller, J. W. *J. Organomet. Chem.* **2002**, *649*, 252.

(63) Evans, W. J.; Bloom, I.; Hunter, W. E.; Atwood, J. L. *Organometallics* **1985**, *4*, 112.

(64) Tilley, T. D.; Andersen, R. A.; Spencer, B.; Ruben, H.; Zalkin, A.; Templeton, D. H. *Inorg. Chem.* **1980**, *19*, 2999.

(65) Evans, W. J.; Hughes, L. A.; Hanusa, T. P. *J. Am. Chem. Soc.* **1984**, *106*, 4270.

(66) Evans, W. J.; Hughes, L. A.; Hanusa, T. P. *Organometallics* **1986**, *5*, 1285.

SiMe₃)₂(THF)₂, **6**,¹⁷ and [(C₅Me₄)SiMe₂(CH₂CH=CH₂)₂Y-(O₂CCH₂SiMe₃)₂]₂, **7**,¹⁷ in which there is no evidence for metal–olefin interaction in the solid state or in solution. Addition of THF to **3** causes only small shifts of the ring and silyl methyl resonances in the ¹H NMR spectrum. The terminal alkene protons remain as a pair of doublets, but they are shifted to δ 4.82 and 4.92 and the multiplet from the internal alkene proton shifts to δ 5.94. Two new peaks of equal intensity corresponding to THF are observed at δ 1.45 and 3.59. Likewise, addition of dimethoxyethane, pyridine, and 2,2-bipyridine to **3** also causes shifting of the terminal and internal alkene proton resonances, Table 1.

In contrast to the ¹H NMR data, the ¹³C NMR spectrum of **3** had some unusual shifts. The ¹³C NMR spectrum contains nine peaks as expected. However, the alkene carbon peaks, at δ 147.6, assignable to the internal carbon, and at δ 107.9, assignable to the terminal carbon, are shifted substantially from the alkene carbon peaks in **6**, δ 136.1 and 113.5, and **7**, δ 136.5 and 112.7. No metal–alkene interaction is observed via ⁸⁹Y–C coupling in **6** and **7**. Addition of THF to **3** in C₆D₆ causes the internal alkene carbon to shift upfield to δ 140.5 ppm and the terminal alkene carbon shifts downfield to 111.0. This is in the direction of the resonances for **6** and **7** and the free ligand, Table 1. Addition of DME, pyridine, and 2,2-bipyridine causes similar shifts in the ¹³C NMR spectra. Hence, it appears that the unusual ¹³C NMR shifts of unsolvated **3** arise from metal–olefin interactions which can be disrupted by the addition of donor solvents. This is further supported by the structural data on the DME adduct of **3** described later.⁶⁸ Variable temperature ¹³C NMR studies on **3** and **3** + THF showed no significant variation of the spectra, even at temperatures as low as –85 °C in C₇D₈. No signal for either alkene carbon resonance is observable past –60 °C in both **3** and **3** + THF.

The NMR spectra of **1** are complicated by the paramagnetic nature of Sm(II), but the following tentative ¹H NMR assignments can be made: ring methyl peaks at δ 6.21 and –0.99, a methyl peak for the Me₂Si bridge at δ 0.51, the CH₂ attached to Si at δ 10.2, and three peaks at δ 42.4, 38.4, and 24.8 in a 1:1:1 ratio assigned to the alkene protons. Upon addition of THF, two new peaks of equal intensity corresponding to coordinated THF are observed at δ 7.30 and –3.08. All of the other peaks shift: the ring methyls to δ 4.10 and 1.03, the silyl methyls to δ 2.33, the CH₂ to δ 11.5, and the alkene protons to δ 36.6, 32.9, and 26.6. The large shifts in the alkene resonances of **1** upon addition of THF are consistent with the shifts for **3** upon addition of donor solvents and could result from displacement of the tethered olefin from the vicinity of the metal. The paramagnetism of [(C₅Me₄)SiMe₂(CH₂CH=CH₂)₂Eu, **2**, precluded detailed NMR analysis.

To obtain more information on the metal–olefin interactions in **1–3**, crystallographic data were sought. Although **1–3** were isolated as waxy solids, single crystals of all three metallocenes were obtainable (Figures 1–3). Complexes **1** and **3** are isomorphous and crystallize with one molecule of toluene in the unit cell. Complex **2** crystallized from hexane without any solvent in the lattice. As shown in Table 2, the metallocene structural parameters of **1** and **2** are similar. The data on **3** are

Table 2. Selected Bond Lengths (Å) and Angles (deg) for [(C₅Me₄)SiMe₂(CH₂CH=CH₂)₂Sm, **1**, [(C₅Me₄)SiMe₂(CH₂CH=CH₂)₂Eu, **2**, [(C₅Me₄)SiMe₂(CH₂CH=CH₂)₂Yb, **3**, and [(C₅Me₄)SiMe₂(CH₂CH=CH₂)₂Sm][BPh₄], **5**

compound	1	2	3	5
Ln(1)–Cnt1 ^a	2.551	2.558	2.437	2.410
Ln(1)–Cnt2 ^b		2.558		2.409
Ln(1)–Cnt3 ^c	3.048	3.086	2.973	2.952
Ln(1)–Cnt4 ^d		3.096		2.993
Ln(1)–C(ring 1) ^e	2.823(3)	2.828(3)	2.720(2)	2.697(3)
Ln(1)–C(ring 2) ^f		2.822(3)		2.697(3)
Ln(1)–C(13)	3.249(4)	3.293(4)	3.182(3)	3.166(3)
Ln(1)–C(14)	3.004(3)	3.008(3)	2.905(3)	2.878(3)
Ln(1)–C(27)		3.243(3)		3.262(3)
Ln(1)–C(28)		3.089(3)		2.854(3)
C(13)–C(14)	1.415(7)	1.328(4)	1.328(5)	1.324(5)
C(27)–C(28)		1.328(4)		1.316(5)
Cnt1–Ln(1)–Cnt2	141.2	140.9	141.9	137.1
C(14)–Ln(1)–C(13)	25.78(13)	23.32(9)	24.66(10)	24.72(9)
C(28)–Ln(1)–C(27)		24.05(8)		23.66(9)
Cnt1–Ln(1)–C(14)	109.1	105.1	107.7	109.7
Cnt1–Ln(1)–C(28)		103.6		105.4
C(14)–C(13)–C(12)	129.9(4)	126.6(4)	126.4(3)	126.9(3)
C(28)–C(27)–C(26)		127.7(3)		126.9(3)

^a Cnt1 is the centroid of the C(1)–C(5) ring. ^b Cnt2 is the centroid of the C(15)–C(19) ring. ^c Cnt3 is the center of C(13)–C(14). ^d Cnt4 is the center of C(27)–C(28). ^e Average of C(1)–C(5). ^f Average of C(15)–C(19).

also similar when the difference in ionic radii is considered (eight coordinate Yb(II) is 0.11 Å smaller than eight coordinate Eu(II)).⁶⁹

In each complex, the metal is coordinated to the two cyclopentadienyl rings in a typical metallocene fashion and no coordinated THF is present. The average Ln–C(cyclopentadienyl ring) distances and the (ring centroid)–Ln–(ring centroid) angles of **1** and **2** are similar to those of (C₅Me₅)₂Sm⁶⁶ and (C₅Me₅)₂Eu,⁶⁶ as shown in Table 3. The parameters for **3** differ slightly from the two unique molecules found in the asymmetric unit for (C₅Me₅)₂Yb:⁴⁵ **3** has a Yb–ring(average) distance 0.05–0.06 Å longer and a (ring centroid)–Yb–(ring centroid) angle 3–4° smaller than those in decamethylterbocene.

Both of the tethered olefins in each complex, **1–3**, are oriented toward the metal center. This provides the first comparative crystallographic data on interactions of the three divalent lanthanides, Eu, Yb, and Sm with olefins. The tethered alkenes approach the metal in an unsymmetrical orientation, with the terminal alkene carbon atoms 0.2–0.3 Å closer than the internal carbons, as shown in Table 4. All of these Ln–C(alkene) distances are longer than the Ln–C(cyclopentadienyl ring) average lengths, as is typical for long distance lanthanide hydrocarbon interactions.^{31,70–72} Long-range intermolecular Ln···C interactions were also observed in the solid state for the analogous permethyl complexes, (C₅Me₅)₂Ln.^{45,66}

The only other structurally characterized divalent lanthanide alkene complex in the literature involves a platinum coordinated ethylene, (C₅Me₅)₂Yb(μ-η²:η²-C₂H₄)Pt(PPh₃)₂, **8**.⁴⁴ The Yb–C(alkene) distances for coordination of the single olefin in **8**, 2.770(3) and 2.793(3) Å, are significantly shorter than those for the two olefins in **3**, 2.905(3) and 3.182 Å. In **8**, the structural parameters of the (C₅Me₅)₂Yb and (C₂H₄)Pt(PPh₃)₂ components were not very different from those of the free entities. Hence, little metal–olefin interaction was revealed by the structure.

(67) Evans, W. J.; Keyer, R. A.; Ziller, J. W. *J. Organomet. Chem.* **1990**, 394, 87.

(68) Crystallographic cell constants for **3**·DME: Hexagonal, space group *P6*₁, *a* = 19.1515(11) Å, *c* = 18.2474(11) Å, *V* = 5796.1(10) Å³.

(69) Shannon, R. D. *Acta Crystallogr., Sect. A.* **1976**, A32, 751.

Table 3. Comparison of Selected Bond Distances (Å) and Angles (deg) for $[(C_5Me_4)SiMe_2(CH_2CH=CH_2)]_2Sm$ (**1**), $(C_5Me_5)_2Sm$, $[(C_5Me_4)SiMe_2(CH_2CH=CH_2)]_2Eu$ (**2**), $(C_5Me_5)_2Eu$, $[(C_5Me_4)SiMe_2(CH_2CH=CH_2)]_2Yb$ (**3**), and $(C_5Me_5)_2Yb$

compound	1	$(C_5Me_5)_2Sm$	2	$(C_5Me_5)_2Eu$	3	$(C_5Me_5)_2Yb$
Ln–C(ring) average	2.823(3)	2.79(1)	2.828(3)	2.79(1)	2.720(2)	2.66
Ln–ring centroid	2.551	2.53	2.822(3)	2.558	2.437	2.67
ring centroid–Ln– ring centroid	141.2	140.1	2.552	140.9	141.9	146
			140.9	140.3		145

Table 4. M–C(alkene) Distances for $[(C_5Me_4)SiMe_2(CH_2CH=CH_2)]_2Sm$ (**1**), $[(C_5Me_4)SiMe_2(CH_2CH=CH_2)]_2Eu$ (**2**), $[(C_5Me_4)SiMe_2(CH_2CH=CH_2)]_2Yb$ (**3**), $\{[(C_5Me_4)SiMe_2(CH_2CH=CH_2)]_2\}Sm[BPh_4]$ (**5**), $(C_5Me_5)_2Yb(\mu-\eta^2:\eta^2-C_2H_4)Pt(PPh_3)_2$ (**8^a**), and $[(C_5Me_5)_2Sm][(\mu-Ph)_2BPh_2]$ (**9^b**)

compound	1	2	3	5	8 ^a	9 ^b
M–C(terminal)	3.004(3)	3.008(3)	2.905(3)	2.854(3)	2.770(3)	3.059(3)
		3.089(3)		2.878(3)		3.175(3)
M–C(internal)	3.249(4)	3.243(3)	3.182(3)	3.166(3)	2.793(3)	2.825(3)
		3.293(4)		3.262(3)		2.917(3)

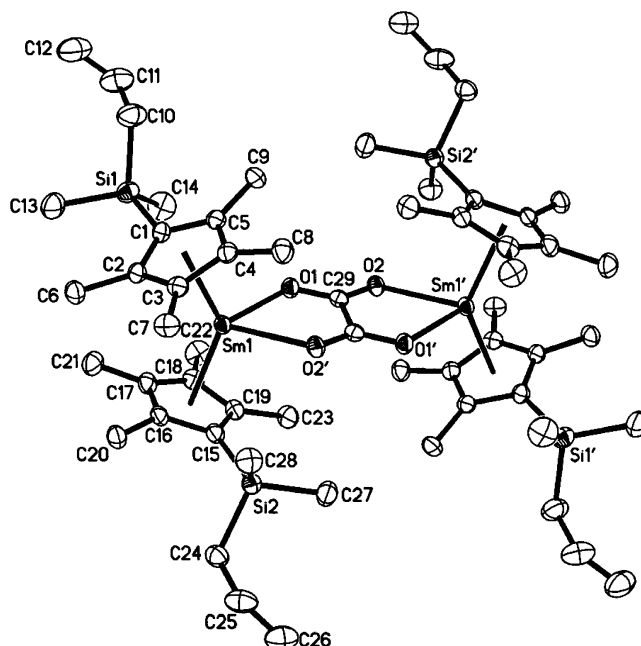
^a The terminal/internal distinction of carbon atoms does not apply in this complex. ^b These are Sm–C(arene) distances.

Since **1–3** have comparatively longer Ln–C distances, these complexes also show only a weak interaction between the two olefins and the metal. Consistent with this, the C(alkene)–C(alkene) distances in **2** and **3**, 1.328(4) and 1.328(5) Å, for C(13)–C(14) and C(27)–C(28), are similar to the 1.283(6) and 1.310(6) Å lengths in **4** (discussed later), in which the alkene is noninteracting. The alkene carbon atoms in **1** have large thermal ellipsoids that may arise from disorder. As a result, a reliable C(alkene)–C(alkene) distance was not obtainable for **1**.

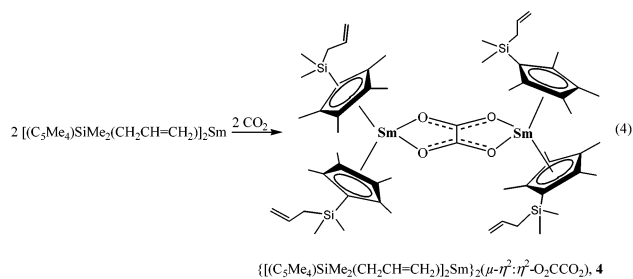
Attempts to crystallize **1–3** in the presence of donor solvents, to have structures of the divalent complexes with the olefin not interacting, were largely unsuccessful. This differs considerably from the $(C_5Me_5)_2Ln$ systems which readily form crystalline $(C_5Me_5)_2LnL_x$ complexes.^{44–45,64–67} However, in the case of $[(C_5Me_4)SiMe_2(CH_2CH=CH_2)]_2Yb$ in the presence of dimethoxyethane, crystals of $[(C_5Me_4)SiMe_2(CH_2CH=CH_2)]_2Yb(DME)$ were obtained which showed coordination of both DME oxygen donor atoms to the metal.⁶⁸ Unfortunately, the structure was not of high enough quality to provide more than connectivity. This structure did show that donor solvents will coordinate to the $[(C_5Me_4)SiMe_2(CH_2CH=CH_2)]_2Ln$ complexes and that this coordination could cause the changes observed in ¹³C NMR shifts upon addition of donor solvent.

Reductive Reactivity of $[(C_5Me_4)SiMe_2(CH_2CH=CH_2)]_2Sm$.

To compare the reactivity of $[(C_5Me_4)SiMe_2(CH_2CH=CH_2)]_2Sm$ with $(C_5Me_5)_2Sm(THF)_2$, the reaction of **1** with CO₂ was examined. $(C_5Me_5)_2Sm(THF)_2$ reductively couples CO₂ to the oxalate dianion, $[(C_5Me_5)_2Sm]_2(\mu-\eta^2:\eta^2-O_2CCO_2)$.⁷³ $[(C_5Me_4)SiMe_2(CH_2CH=CH_2)]_2Sm$ reacts similarly with CO₂ in minutes in hexanes to form a yellow-orange product, **4**, which was identified by X-ray crystallography as the direct analogue

**Figure 4.** Thermal ellipsoid plot of $\{[(C_5Me_4)SiMe_2(CH_2CH=CH_2)]_2Sm\}_2(\mu-\eta^2:\eta^2-O_2CCO_2)$, **4**, with ellipsoids drawn at the 50% probability level.

$\{[(C_5Me_4)SiMe_2(CH_2CH=CH_2)]_2Sm\}_2(\mu-\eta^2:\eta^2-O_2CCO_2)$, eq 4. Complex **4** is isolated in 95% yield.



The color and ¹H and ¹³C NMR spectra of **4** were consistent with formation of a trivalent samarium complex. Resonances attributable to the terminal protons of the tethered CH₂CH=CH₂ group were found as doublets at δ 4.00 and 4.22 ppm. The proton on the internal carbon was located as a multiplet at δ 4.73. The ¹³C spectrum contains nine peaks as expected for the cyclopentadienyl ligand, and an additional resonance is observed at δ 199 ppm which could be assigned to the quaternary carbons of the oxalate bridge. The terminal and internal alkene carbon resonances were found at δ 112.1 and 133.5, respectively.

The structure of **4**, Figure 4, which is similar to that of $[(C_5Me_5)_2Sm]_2(\mu-\eta^2:\eta^2-O_2CCO_2)$,⁷³ provides the first detailed

(70) Evans, W. J.; Giarikos, D. G.; Robledo, C. B.; Leong, V. S.; Ziller, J. W. *Organometallics* **2001**, *20*, 5648.

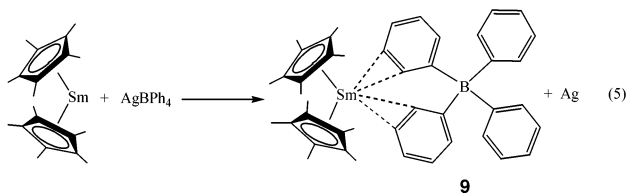
(71) Evans, W. J.; Ulibarri, T. A.; Ziller, J. W. *J. Am. Chem. Soc.* **1990**, *112*, 219.

(72) Evans, W. J.; Gonzales, S. L.; Ziller, J. W. *J. Am. Chem. Soc.* **1994**, *116*, 2600.

(73) Evans, W. J.; Seibel, C. A.; Ziller, J. W. *Inorg. Chem.* **1998**, *37*, 770.

structural information on this metallocene oxalate, since the data on the C_5Me_5 analogue were not of high quality. The alkene functionalities on the rings are oriented away from the metal with C(alkene)–C(alkene) distances of 1.283(6) and 1.310(6) Å. The tetradentate oxalate dianion, $[O_2CCO_2]^{2-}$, bridges the two Sm atoms by formation of two five-membered SmOCCO rings, a typical coordination mode for the oxalate anion.^{73–76} The oxalate ligand is planar, as indicated by the angles about C(29), and the 1.560(6) Å C(29)–C(29') bond is normal for a single bond.⁷⁷ The 2.400(2) Å Sm(1)–O(1) and 2.398(2) Å Sm(1)–O(2') distances in **4** are longer than the 2.303(4)–2.317(4) Å Sm–O range found in the bridging carboxylate dimers, $[(C_5Me_5)_2Sm(\mu-O_2CCH_2CH=CH_2)]_2$ and $[(C_5Me_5)_2Sm(\mu-O_2CC_6H_5)]_2$, which contain eight-membered SmOCO SmOCO rings.⁷⁸ The Sm–O distances in **4** are also longer than the Sm–O distance of 2.30(1) Å found in $(C_5Me_5)_2Sm[\mu-\eta^4-(PhN)OCCO(NPh)]Sm(C_5Me_5)_2$, which also contains five-membered rings and eight-coordinate samarium centers counting each six-electron $C_5Me_5^-$ ligand as occupying three coordination sites.⁷⁹ However, the Sm–O distances in **4** are shorter than those found with neutral oxygen donor ligands in eight-coordinate trivalent samarium systems, which range from 2.44(2)–2.511(4) Å.⁸⁰

Formation of a Cationic Species. To obtain a cationic species to test the tethered alkene versus $[BPh_4]^-$ anion coordination issue, a reaction analogous to the $(C_5Me_5)_2Sm/AgBPh_4$ system, eq 5, was examined. Like $(C_5Me_5)_2Sm$,



$[Me_2Si(C_5Me_4)(CH_2CH=CH_2)]_2Sm$ reacts with $AgBPh_4$ in toluene. The dark green color transforms over 12 h to a dark red product, **5**, with the formation of a black precipitate. The 1H NMR and ^{13}C NMR spectra of **5** are not informative due to the poor solubility of the complex. The 1H NMR spectrum contains a broad singlet at $\delta -1.33$ ppm that could be assigned to one set of the ring methyls, but a resonance for the other set was not identifiable. In comparison, the ring methyl protons in $[(C_5Me_5)_2Sm][(\mu-Ph)_2BPh_2]$, **9**, were observed at $\delta -0.34$ ppm. A second broad singlet in the spectrum of **5** at $\delta 7.78$ ppm was observed and can be assigned to the phenyl protons of the tetraphenylborate anion. A peak at $\delta 8.4$ ppm was observed in the spectrum of **9**.

The IR spectrum of **5** is similar to those of **1–3**, except that absorbances attributable to the tetraphenylborate anion (similar to absorptions observed for **9**) are observed and the strong absorbance at 1629 cm^{-1} for the C=C stretch observed for **1–3**

(74) Guillou, O.; Bergerat, P.; Kahn, O.; Bakalbassis, E.; Boubekeur, P.; Batail, P.; Guillot, M. *Inorg. Chem.* **1992**, *31*, 110.

(75) Huang, S.; Zhou, G.; Mak, T. C. W. *J. Crystallogr. Spectrosc. Res.* **1991**, *21*, 127.

(76) Kahwa, I. A.; Fronczek, F. R.; Selbin, J. *Inorg. Chim. Acta* **1994**, *82*, 161.

(77) Allen, F. H.; Kennard, O.; Watson, D. G.; Brammer, L.; Orpen, A. G.; Taylor, R. *J. Chem. Soc., Perkin Trans. 2* **1987**, S1.

(78) Evans, W. J.; Seibel, C. A.; Ziller, J. W.; Doedens, R. *J. Organometallics* **1998**, *17*, 2103.

(79) Evans, W. J.; Drummond, D. K. *J. Am. Chem. Soc.* **1986**, *108*, 7440.

(80) Evans, W. J.; Foster, S. E. *J. Organomet. Chem.* **1992**, *433*, 79.

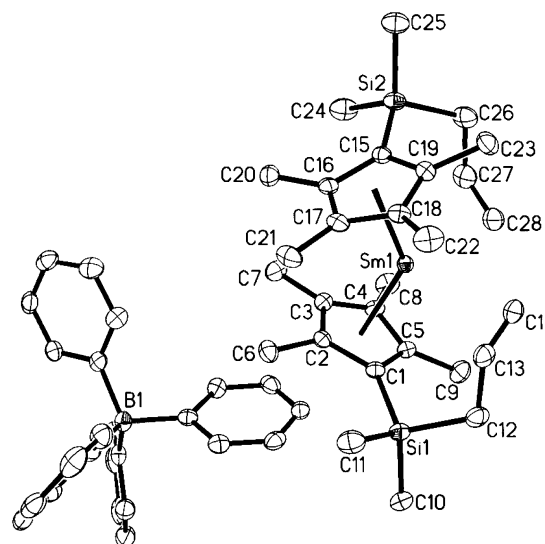


Figure 5. Thermal ellipsoid plot of $\{[(C_5Me_4)SiMe_2(CH_2CH=CH_2)]_2Sm\}[BPh_4]$, **5**, with ellipsoids drawn at the 50% probability level.

is not present. To gain more definitive evidence on the alkene versus $[BPh_4]^-$ coordination question, an X-ray crystallographic study was conducted.

X-ray crystallography confirmed the composition of $\{[(C_5Me_4)SiMe_2(CH_2CH=CH_2)]_2Sm\}[BPh_4]$ for **5**, which is analogous to the permethyl product **9** obtained in eq 5. However, X-ray crystallography also revealed that, unlike $(C_5Me_5)_2Sm(\mu-Ph)_2BPh_2$, in which the $[BPh_4]^-$ anion is oriented toward samarium through two of the arene rings, eq 5, the $[BPh_4]^-$ ion in **5** is not interacting with the metal. Instead, both pendant olefins are oriented toward the Sm(III) center, Figure 5, eq 6.

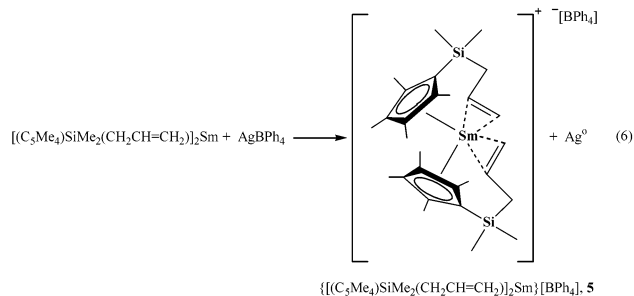


Table 5 summarizes a comparison of selected bond lengths and angles for **5**, $(C_5Me_5)_2Sm(\mu-Ph)_2BPh_2$, and $[(C_5Me_5)_2Sm(THF)_2][BPh_4]$.²⁵ The metrical parameters for the metallocene part of **5** are not significantly different from those of the other compounds. Similar to **1–3**, the alkenes in **5** are oriented toward samarium in an unsymmetrical fashion with the 2.854(3) and 2.878(3) Å Sm–C(terminal alkene) distances shorter than the 3.166(3) and 3.262(3) Å Sm–C(internal alkene) distances. These Sm–C distances are shorter than those in **1** as expected for a Sm(III) versus Sm(II) system. These Sm–olefin distances can also be compared with the four closest Sm–C(arene) distances in trivalent **9**: 2.825(3), 2.917(3), 3.059(3), and 3.175(3) Å. The 1.324(5) and 1.316(5) Å C(alkene)–C(alkene) distances in **5** are indistinguishable from the C(alkene)–C(alkene) distances in **2–4**.

Discussion

The $[(C_5Me_4)SiMe_2(CH_2CH=CH_2)]^-$ ligand, the neutral metallocenes **1–3**, and the cationic metallocene **5** are well suited

Table 5. Comparison of Selected Bond Distances (Å) and Angles (deg) for $\{[(C_5Me_4)SiMe_2(CH_2CH=CH_2)]_2Sm\}[BPh_4]$ (**5**), $[(C_5Me_5)_2Sm][(\mu-Ph)_2BPh_2]$ (**9**), and $[(C_5Me_5)_2Sm(THF)_2][BPh_4]$, **10**

compound	5	9	10
ring centroid–Sm–ring centroid	137.1	134.4(2)	134.2
Sm–ring centroid	2.410	2.420	2.423
	2.409	2.422	
Sm–C(ring) range	2.630(3)–2.746(3)	2.670(3)–2.740(3)	2.66(3)–2.71(2)
Sm–C(ring) average	2.697(3)	2.70(2)	2.69(2)
Sm–C(L) ^a	2.878(3)	2.825(3)	
	3.166(3)	3.059(3)	
	2.854(3)	2.917(3)	
	3.262(3)	3.175(3)	

^a L is alkene for **5** and arene for $[(C_5Me_5)_2Sm][(\mu-Ph)_2BPh_2]$.

for studying metal–alkene chemistry in a metallocene environment. The tethered olefin can function simply as an ancillary cyclopentadienyl substituent as seen in **4**, $\{[(C_5Me_4)SiMe_2(CH_2CH=CH_2)]Y(O_2CCH_2SiMe_3)_2\}_2$,¹⁷ **6**, and $[(C_5Me_4)SiMe_2(CH_2CH=CH_2)]Y(CH_2SiMe_3)_2(THF)_2$,¹⁷ **7**, in which it is not interacting with the metal. Alternatively, as demonstrated by **1–3** and **5**, it can function as a chelating ligand with which metal–olefin coordination can be studied. It also can be a reactant in metalation chemistry, as demonstrated by the formation of $\{[(C_5Me_4)SiMe_2(C_3H_3)]Y(L)\}_2$ (L = THF, DME) from **7**.¹⁷

The synthesis of lanthanide metallocenes of $[Me_2Si(C_5Me_4)(CH_2CH=CH_2)]^-$ is similar to the preparation of the $(C_5Me_5)^-$ analogues except that complexes **1–3** can be isolated from preparations in THF in a form free of coordinating solvents. This is a great advantage, since desolvation of $(C_5Me_5)_2Ln(THF)_x$ is not particularly facile.^{45,66}

Presumably, the origin of the desolvated nature of **1–3** is the presence of the tethered olefin, since the olefin is oriented toward the metal in the solid state. Shifts in the NMR spectra of **1** and **3** in solution can also be interpreted as evidence for tethered olefin coordination. In **1**, the alkene proton resonances are shifted downfield to δ 43.9, 39.8, and 25.5 ppm, indicating that the olefin may be nearby the paramagnetic Sm(II) ion. In **3**, a large shift in the ¹³C NMR spectrum is observed for the internal (Δ = 12.1 ppm) and terminal (Δ = 5.8 ppm) alkene carbons compared to those of the free diene $(C_5Me_4H)SiMe_2(CH_2CH=CH_2)$ and diamagnetic complexes **6** and **7**. These differences are similar to those reported for the ¹³C alkene differences of the chelating $(C_5Me_5)_2Y[\eta^1-CH_2CH_2C(CH_3)_2-CH=CH_2]$ complex, **11**, and its free ligand 3,3-dimethyl-1,4-pentadiene,¹⁰ Table 1. However, THF would be expected to be a better donor and could displace the olefin. Consistent with this, addition of THF to **1** and **3** causes shifts in the proton and carbon resonances of the olefin in both complexes. Similar shifting in the ¹H and ¹³C NMR is seen when the THF solvate is formed from complex **11**. However, it would be expected that the THF would remain solvated and THF adducts would be isolated. This suggests that the tethered olefin is displaceable, but it can protect the metal center from solvation upon crystallization.

The syntheses of **1** and **2** provided the first crystallographically characterized olefin complexes of samarium and europium. Olefin complexes of lanthanide ions are rare, since these hard ionic metals typically do not favor coordination of soft bases. Metal vapor^{46,47} and FTICR^{48–50} studies have provided evidence of interactions between olefins and lanthanide metals in the gas phase, and in solution, an NMR study of $(C_5Me_5)_2Eu$ ⁶⁶ and

ethylene has been reported.⁸¹ However, solid state evidence for such a complex has been lacking. The only other structurally characterized divalent lanthanide olefin complex in the literature involves an olefin already coordinated to another metal, namely the $(C_5Me_5)_2Yb(\mu-\eta^2:\eta^2-C_2H_4)Pt(PPh_3)_2$ complex, **8**, made from $(C_5Me_5)_2Yb$ and $(C_2H_4)Pt(PPh_3)_2$.⁴⁴ In **8**, both components remain similar in structure to the uncomplexed precursors. $(C_5Me_5)_2Sm$ is also known to form crystallographically characterizable π complexes with olefins, but these typically involve reductive complexation of these substrates due to the strong reduction potential of Sm(II).^{70–72,82}

The structures of the three complexes, **1–3**, are similar, as shown in Table 2. In addition, their structural parameters are similar to those of the permethyl analogues, $(C_5Me_5)_2Ln$, Table 3. This is reasonable, since both sets of bent metallocene complexes have additional metal–ligand interactions in the solid state to compensate for their coordinative unsaturation. The solid-state structures of the base-free bent metallocenes $(C_5Me_5)_2Sm$,³¹ $(C_5Me_5)_2Yb$,⁴⁵ $(C_5Me_4H)_2Yb$,⁴⁵ and $[(1,3-(Me_3Si)_2C_5H_3)]_2Yb$ ⁴⁵ show that intermolecular interactions occur which reduce the coordinative unsaturation. In $[1,3-(^tBu)_2C_5H_3]_2Yb$, an intramolecular Yb–ring Me interaction is found.⁴⁵ Complexes **1–3** use the tethered olefins to fill the coordination sphere of the metal in the solid state.

Comparison of the metrical data for **1–3** and **8** suggest that the metal–olefin interactions in **1–3** are not strong. The Ln–C(alkene) distances to the two olefins in **3** are significantly longer than those to the single olefin in **8**. Since the olefin in **8** was not perturbed significantly by the ytterbium, both ytterbium complexes **3** and **8** represent systems of weak interaction. A similar conclusion can be drawn for **1** and **2**, since the metal–olefin distances in **1**, **2**, and **3** are just as expected based on the differences in radii of divalent ions.⁶⁹

Since $(C_5Me_5)_2Sm$ can reduce dinitrogen,⁸³ styrene,⁷⁰ stilbene,⁷⁰ and propene⁸² and it initiates polymerization of ethylene presumably by a reductive route,²¹ reduction of the tethered olefin was possible. However, the dark green color and NMR spectra of **1** are consistent with an Sm(II) rather than an Sm(III) product; that is, they give no evidence of reduction of the tethered olefins. This is also supported by infrared spectroscopy: complexes **1–3** display almost identical spectra, including the terminal C=C stretch observed at 1629 cm⁻¹ for each complex.

(81) Nolan, S. P.; Stern, D.; Marks, T. J. *J. Am. Chem. Soc.* **1989**, *111*, 7844.

(82) Evans, W. J.; Ulibarri, T. A.; Ziller, J. W. *J. Am. Chem. Soc.* **1990**, *112*, 2314.

(83) Evans, W. J.; Ulibarri, T. A.; Ziller, J. W. *J. Am. Chem. Soc.* **1988**, *110*, 6877.

The reactivity of **1** with CO₂, ethylene, and AgBPh₄ indicates that it has chemical behavior similar to its C₅Me₅ analogue. This is not unexpected, since **1** is structurally similar and the olefins are not strongly interacting. Since the reactivities of **1** and (C₅Me₅)₂Sm were similar, the AgBPh₄ reaction was likely to set up a situation in which there could be a competition for the cationic metal site between the arene rings of the tetraphenylborate and the tethered olefins.

The structure of the unsolvated cationic complex, $\{[(C_5Me_4)SiMe_2(CH_2CH=CH_2)]_2Sm\}[BPh_4]$, **5**, indicates that, in the solid state, coordination of the tethered olefins is favored over the tetraphenylborate anion. This preference is somewhat surprising considering that the anionic [BPh₄][−] is known to coordinate to cationic metal centers^{18,84} and olefin coordination is expected to be weak. In fact, in (C₅Me₅)₂Sm(μ -Ph)₂BPh₂,¹⁸ one of the Sm–C(arene ring of BPh₄) bonds, 2.825(3) Å, is shorter than the shortest analogous bond in **5**, which is 2.854(3) Å.

It is possible that the presence of the tethered olefin near the metal rather than the [BPh₄][−] group is due to crystal packing factors. Nevertheless, the structure of **5** demonstrates that there is an environment in which an olefin is preferentially oriented toward the metal compared to [BPh₄][−]. This may well be the case at the active site of the best catalysts.

The structures of **1–3** and **5** allow the first comparison of the interaction of an olefin with a neutral divalent lanthanide complex versus a cationic trivalent lanthanide system. It could be expected that the cationic trivalent system, which is more electrophilic, would lead to tighter binding. On the other hand, the neutral divalent system is a softer metal which may favor coordination of the soft olefin ligand. The comparison will be made between **5** and **2**, since they have indistinguishable C=C distances in the tethered olefin. Since eight-coordinate Sm(III) is 0.171 Å smaller than eight-coordinate Eu(II) according to Shannon radii,⁶⁹ the distances equivalent to the 3.004(3) and 3.089(3) Å Eu(II)–C terminal carbon distances and 3.243(3) and 3.293(4) Å internal carbon distances in **2** would be expected to be 2.837–2.918 Å (terminal) and 3.072–3.122 Å (internal) in **5** if the binding were similar. The analogous terminal carbon distances in **5**, 2.854(3) and 2.878(3) Å, are in this range. However, the 3.166(3) and 3.262(3) Å internal carbon distances are both longer than these extrapolated values. Hence, in terms of the closest interaction of the olefin with metals, that is, the terminal carbon, the divalent and trivalent systems appear to be similar. This might be expected for ionic systems in which there was no significant back-bonding: the distances are equivalent when the size of the metal ion is considered. The importance of the longer internal carbon metal distances in the trivalent **5** is not clear.

One other point that bears discussion is the orientation of the olefin. In **1–3** and **5**, the terminal carbon is closer to the metal than the internal carbon. This is not the case in the simple potassium salt, $[(C_5Me_4)Me_2Si(CH_2CHCH_2)K(THF)]_n$,⁶² but this is found in the cationic Zr(IV) complexes, $[(C_5H_5)_2Zr(OCMe_2CH_2CH_2CH=CH_2)]^+$ and $[(S,S,R)-(EBI)Zr(OCMe_2CH_2CH_2CH=CH_2)]^+$ (EBI = ethylene-1,2-bis(1-indenyl)), which contain alkene ligands tethered via alkoxides.¹⁴ Jordan has proposed two explanations for this similar orientation. One explanation is that this orientation allows the positive charge on the metal to be dispersed onto the internal alkene carbon, thus giving rise to two resonance structures. The electrostatic repulsion between the metal and buildup of partial charge on the internal carbon results in an elongated interaction. This was in agreement with the observed ¹³C data. A substantial shift ($\Delta = 12.1$ ppm) of the internal alkene carbon peak is also observed for **3**. Another explanation involves overlap of the π -bonding orbital on the terminal carbon with a Zr σ -acceptor orbital. A similar explanation could pertain here except that the distances are much longer and the orbital interactions are expected to be much less for lanthanide systems.

Conclusion

The $[(C_5Me_4)Me_2Si(CH_2CH=CH_2)]^-$ ligand has proven again to be useful in investigating metal–olefin interactions in a metallocene environment. In this case, the use of the $[(C_5Me_4)SiMe_2(CH_2CH=CH_2)]^-$ ligand with neutral and cationic lanthanide metallocenes has shown that tethered olefins can interact preferentially with the metal center compared to [BPh₄][−] under certain circumstances. If such a preference exists in some catalytic olefin polymerization systems, this would provide the optimum catalyst. These compounds also demonstrate that lanthanide metallocene chemistry can be significantly affected by the attachment of an alkene functional group to the commonly used polyalkylcyclopentadienyl ligand. The tethered olefin can make it easier to access metallocenes which are not coordinated to solvents or counteranions and can allow olefin complexes of lanthanides to be studied in solution and in the solid state.

Acknowledgment. For support of this research, we thank the Division of Chemical Sciences, Geosciences and Biosciences, Office of Basic Energy Sciences, Office of Sciences, U.S. Department of Energy.

Supporting Information Available: X-ray diffraction data, atomic coordinates, thermal parameters, and complete bond distances and angles; listing of observed and calculated structure factor amplitudes for compounds **1**, **2**, **3**, **4**, and **5** (PDF). This material is available free of charge via the Internet at <http://pubs.acs.org>.

JA020957X

(84) Evans, W. J.; Nyce, G. W.; Forrestal, K. J.; Ziller, J. W. *Organometallics* **2002**, *21*, 1050.